Research article

A three-DOF compliant micromotion stage with flexure hinges

Tien-Fu Lu
Daniel C. Handley
Yuen Kuan Yong and
Craig Eales

The authors

Tien-Fu Lu, **Daniel C. Handley**, **Yuen Kuan Yong** and **Craig Eales** are based at the School of Mechanical Engineering, University of Adelaide, Adelaide, Australia.

Keywords

Microcontrollers, Actuators

Abstract

Micromanipulation has enabled numerous technological breakthroughs in recent years, from advances in biotechnology to microcomponent assembly. Micromotion devices commonly use piezoelectric actuators (PZT) together with compliant mechanisms to provide fine motions with position resolution in the nanometre or even sub-nanometre range. Many multiple degree of freedom (DOF) micromotion stages have parallel structures due to better stiffness and accuracy than serial structures. This paper presents the development of a three-DOF compliant micromotion stage with flexure hinges and parallel structure for applications requiring motions in micrometres. The derivation of a simple linear kinematic model of the compliant mechanism is presented and simulation results before and after calibration are compared with results from finite element (FE) modeling and experiments. The position control system, which uses an experimentally determined constant-Jacobian, and its performance are also presented and discussed.

Electronic access

The Emerald Research Register for this journal is available at
www.emeraldinsight.com/researchregister

The current issue and full text archive of this journal is available at
www.emeraldinsight.com/0143-991X.htm

Industrial Robot: An International Journal
Volume 31 · Number 4 · 2004 · pp. 355–361
 · ISSN 0143-991X
DOI 10.1108/01439910410541873

1. Introduction

Owing to increasing demand the research of micromanipulation systems has become more intense in recent years. Possible applications include microsystem assembly, biological cell manipulation and microsurgery. One common need is to manipulate microscale objects and to perform very small motions, say less than 100 μm, with good positioning accuracy. Conventional technologies based on servomotors, ball screws, and rigid linkages struggle to fulfil these requirements due to inherent problems, such as clearance, friction and backlash. Therefore, compliant mechanisms with parallel structures, flexure hinges and novel actuators, such as piezoelectric actuators, have been adopted in many designs of micromotion devices (Gao *et al.*, 1999; Ryu *et al.*, 1997; Scire and Teague, 1978). Compliant mechanisms generate their motions through elastic deformations and replace the joints in rigid mechanisms by flexure hinges. These mechanisms are advantageous over the rigid-link designs in applications requiring micromotion (Howell, 2001) because problems such as friction, wear, backlash and lubrications are eliminated. Furthermore, compliant mechanisms contain fewer components compared to rigid-body mechanisms, thus allowing for savings in weight. In terms of parallel structure, all the actuators can be located at the base, thus reducing the active mobile mass (Codourey, 1998) and leading to higher loading capacity. Parallel structures also have higher mechanical stiffness, faster manipulation and higher positioning accuracy (Ma and Angeles, 1993). These characteristics are beneficial for micromotion devices.

Scire and Teague (1978) developed one of the earliest compliant micromotion stages for use in electron microscopes. Their one degree of freedom (DOF) stage consisted of flexure pivoted lever arms to amplify the linear displacements of the PZT actuator. Gao *et al.* (1999) designed a two-DOF piezodriven precision micropositioning stage utilising flexure hinges. The design adopted two amplifying levers and a monolithic symmetrical mechanism. Ryu *et al.* (1997) developed a $XY\theta$ micropositioning stage consisting of a monolithic flexure hinge mechanism with PZT actuators. This was optimally designed to provide maximum rotation.

In order to deal in a systematic and efficient way with problems involving the time-dependent behaviour of micromotion stages, accurate models are required. These models are used for analysis to predict the system performance and for controller design to achieve successful operation under changing conditions. However, to achieve

Industrial Robot: An International Journal
Volume 31 · Number 4 · 2004 · 355–361

real-time control, especially for higher frequency operations, simpler models that incur less computation are essential. When deriving models, complex kinematics will lead to even more complicated dynamic models. Thus, we look into kinematics as a starting point to find ways of deriving simpler dynamic models. Of course, although computationally less efficient, accurate kinematic models are still useful to achieve good positioning control for many applications, such as microsurgery, biological cell manipulation and microassembly.

This paper first presents the design and structure of the 3RRR compliant micromotion stage, and its linear kinematics. Then, the simulation environment and experimental set-up are described. Following this description, simulation results before and after calibration obtained from the derived simplified linear kinematic model is compared with results from finite element (FE) modeling and experiments. The control system of the micromotion stage is then discussed. Open and closed loop controls that are based on an experimentally determined constant-Jacobian are introduced and their performance for position control are presented and discussed. Finally, conclusions are drawn and future work discussed.

2. The micromotion stage design

The micromotion system presented in this study is a three-DOF parallel micromotion stage (also known as a 3RRR [1] compliant mechanism). It is a monolithic compliant mechanism utilising flexure hinges. The stage is actuated by three PZT stack actuators as shown in Figure 1 and is designed based on the 3RRR mechanism structure as shown in Figure 2. The end-effector platform is attached to the ends of the three linkages as illustrated by a triangle in Figure 1.
The end-effector translates along x, y-axis and rotates about the z-axis. This type of parallel compliant mechanism amplifies the motion of the PZT actuators. Its monolithic structure makes the manufacturing process simple and also cost-effective. It does not require the assembly of multiple stages to achieve three-DOF and therefore is compact and light in weight.

3. Linear kinematic model

The pseudo-rigid-body model approach and loop-closure theory are adopted for the derivations of linear kinematics (Yong *et al.*, 2004).
The pseudo-rigid-body model (PRBM) is used to model the deflections of the flexible members using conventional rigid-link mechanism theory (Howell, 2001). The PRBM assumes that the flexure hinges in the structure act like revolute joints with torsional springs attached to them. The other parts of the structure are assumed to be rigid. Therefore, the PRBM is referred to as a bridge connecting the rigid-link mechanism and the compliant mechanism (Howell, 2001). The PRBM of the presented 3RRR compliant mechanism is shown in Figure 2. Loop-closure theory incorporates the complex number method to model a mechanism. For each closed-loop in the mechanism, a loop equation is generated (Howell and Midha, 1996). This equation can be expressed in terms of its real and imaginary parts, resulting in two equations per loop. Unknowns can be found by solving these equations simultaneously.

In Figure 2, all the flexure hinges labelled A_i are actuated (active joints). Flexure hinges B_i and C_i are unactuated (passive joints). Therefore, $\Delta\theta_{Bi}$ and $\Delta\theta_{Ci}$ ($i = 1, 2, 3$) are unknowns. In order to

Figure 1 The 3RRR compliant micromanipulation device

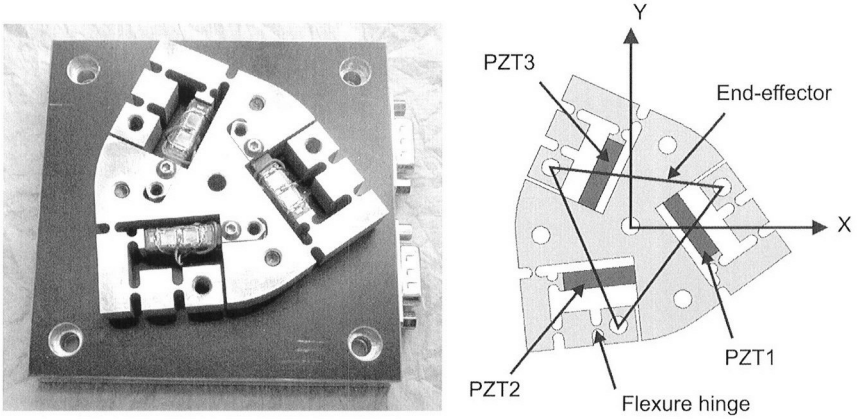

Industrial Robot: An International Journal
Volume 31 · Number 4 · 2004 · 355–361

Figure 2 The 3RRR compliant mechanism

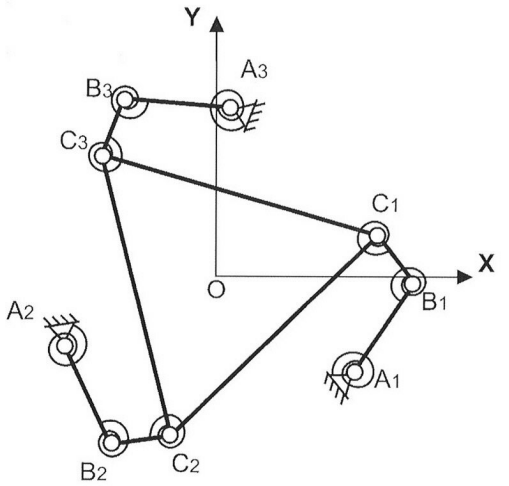

solve these six unknowns, three closed-loops are generated. Using the loop-closure theory, six equations can be obtained. As the angular displacements of the mechanism are small, linear small angle approximations can be used. The six equations obtained are linear and can be solved simultaneously to obtain the unknown angular displacement increments without requiring iteration techniques. These unknowns are expressed in terms of the input displacements of the PZT actuators, Δl_i ($i = 1, 2, 3$), as:

$$\Delta\theta_B = \begin{bmatrix} \Delta\theta_{B1} \\ \Delta\theta_{B2} \\ \Delta\theta_{B3} \end{bmatrix} = \begin{bmatrix} 481 & 320 & -190 \\ -190 & 481 & 320 \\ 320 & -190 & 481 \end{bmatrix} \begin{bmatrix} \Delta l_1 \\ \Delta l_2 \\ \Delta l_3 \end{bmatrix} \quad (1)$$

$$\Delta\theta_C = \begin{bmatrix} \Delta\theta_{C1} \\ \Delta\theta_{C2} \\ \Delta\theta_{C3} \end{bmatrix} = \begin{bmatrix} -255 & -380 & 130 \\ 130 & -255 & -380 \\ -380 & 130 & -255 \end{bmatrix} \begin{bmatrix} \Delta l_1 \\ \Delta l_2 \\ \Delta l_3 \end{bmatrix} \quad (2)$$

By knowing all the unknown angular displacements of the flexure hinges, the forward kinematics can be derived easily. Mathematically, forward kinematics is derived to find the positions and orientations (Δx, Δy, $\Delta\gamma$)[2] of the end-effector when the actuated joint variables (Δl_1, Δl_2, Δl_3) are given. A Jacobian matrix is normally used to relate the velocity of an end-effector to the velocity of actuators. However, for the case of compliant micromotion stages, the Jacobian matrix can be defined as a matrix to relate (Δl_1, Δl_2, Δl_3) with (Δx, Δy, $\Delta\gamma$) (Zhang *et al.*, 2002) (equation (3)). The displacements of the PZT actuators are small compared to the link lengths and the motions of the 3RRR mechanism are very small. Therefore, the micromanipulation stage is almost configurationally invariant and its Jacobian matrix is assumed to be constant.

$$\begin{bmatrix} \Delta x \\ \Delta y \\ \Delta\gamma \end{bmatrix} = \mathcal{J} \begin{bmatrix} \Delta l_1 \\ \Delta l_2 \\ \Delta l_3 \end{bmatrix} \quad \text{where}$$

$$\mathcal{J} = \begin{bmatrix} 1.905 & -3.22 & 1.315 \\ -2.618 & -0.341 & 2.96 \\ -59.96 & -59.96 & -59.96 \end{bmatrix} \quad (3)$$

Using the linear kinematics, the dynamic model of this compliant mechanism has also been derived (Handley *et al.*, 2004). The theoretical stiffness of the compliant micromotion stage is given in equation (4).

$$K = \begin{bmatrix} 30.7\times10^6 & 759{,}063 & 759{,}063 \\ 759{,}063 & 30.7\times10^6 & 759{,}063 \\ 759{,}063 & 759{,}063 & 30.7\times10^6 \end{bmatrix} \quad (4)$$

4. Simulation and experimental set-up

The simulations were carried out using MATLAB for the full and simplified linear forward kinematic models. The finite element analysis was carried out using ANSYS with a solid model of the micromotion stage built as shown in Figure 3. The FEA model includes the modelling of the compliant mechanism, end-effector platform, PZT actuators and three bolts, which hold the platform to the compliant mechanism.

The experimental set-up of the micromotion system consists of three Tokin AE0505D16 PZT stack actuators assembled into a flexure hinge, compliant mechanism, as shown in Figure 1. Each unloaded actuator has a maximum displacement of approximately 15 μm. These PZTs are each driven by a Physik Instrumente (PI) PZT amplifier, which provides a bi-polar voltage ranging from -20 to 120 V. The amplifiers have a maximum output power of 30 W. Measurement Group EA-06-125TG-350 strain gauges are mounted to the PZTs to determine their displacement. All the strain gauges are connected to a strain gauge conditioner. The end-effector location is measured using three Micro-Epsilon eddyNCDT 3700 eddy-current transducers. The PZT amplifiers, strain gauge conditioning circuitry and eddy-current transducers are connected to a dSPACE DS1104 DSP controller board via inbuilt DACs and ADCs. A schematic of the experimental set-up is shown in Figure 4.

Figure 3 The FEA model of the 3RRR compliant micromotion stage

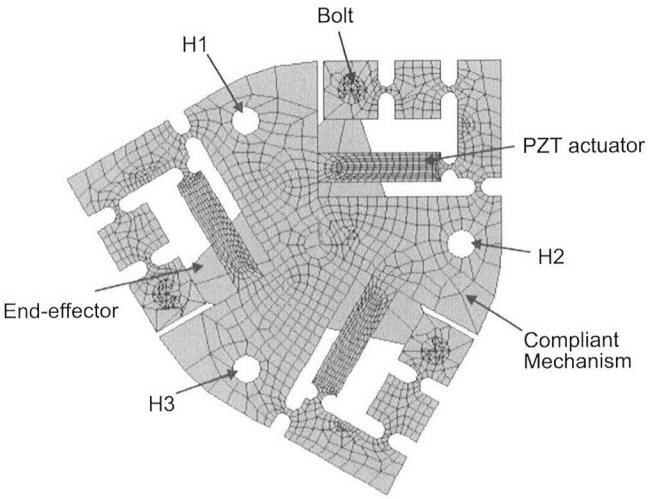

Figure 4 Schematic of the experimental set-up

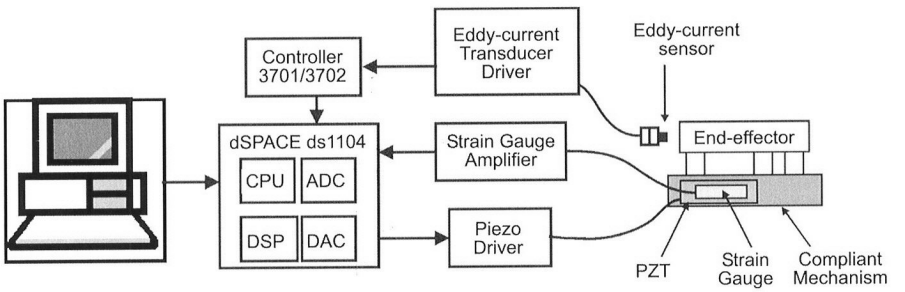

5. Comparison of results

Figure 5 plots the experimental and all the simulation results for comparison including solutions obtained from the full forward kinematic model (Zhang *et al.*, 2002), the derived linear kinematic model before and after calibration, the finite element analysis and the experiments. Figure 5 is obtained by extending PZT1 from 0 to 10 μm with 1 μm increment, and PZT2 and PZT3 are not extended (0 μm). Similarly, PZT2 and PZT3 were also extended, respectively, to obtain other sets of data that have similar result but are not presented here.

Table I exhibits the maximum difference of the positions and orientations at the end-effector between the linear kinematic model and a standard non-linear kinematic model. It can be seen from Table I that the difference between two models are very small and can be neglected for many applications. Therefore, the linear kinematic model derived can be used to replace the non-linear kinematic model.

As can be seen from Figure 5, even though the results from the non-linear kinematic model and the derived linear model are nearly identical, they are not close to the experimental results. This can be attributed to the fact that these two kinematic models have not accounted for other factors, such as the compliance of the flexure hinges in directions other than the rotational axis of the joint, which could be a major source of errors. There is also the possibility of compliance in the mechanism at the base of the PZT. To close the big gaps between the results from experiments and the derived model, calibration was carried out and consequently the results are largely improved but still with noticeable errors. Nevertheless, the FEA model so far has produced good results and will be fine-tuned to match better with experimental results.

With noticeable errors after calibration, the calibrated kinematic model still cannot be used to predict or analyze system performance for position control with satisfactory accuracy for many applications. Therefore, an experimental constant Jacobian is obtained out of the experimental data to relate the extensions of PZTs with the end-effector movement. The experimental Jacobian matrix that converts extensions of PZTs to end-effector movement (forward kinematics) and its inverse matrix (inverse kinematics) are then

Figure 5 Results comparison with only PZT1 input

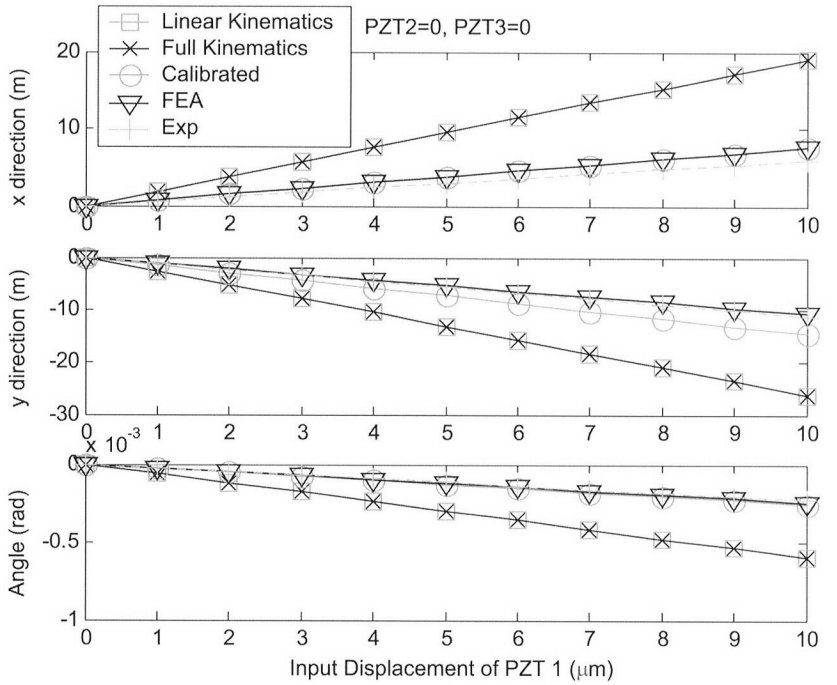

Table I Maximum errors of the positions and orientations

	Maximum errors					
	PZT1 extended		PZT2 extended		PZT3 extended	
	Absolute	Per cent	Absolute	Per cent	Absolute	Per cent
Δx	23.10 nm	1.012×10^{-7}	29.21 nm	1.847×10^{-7}	6.11 nm	1.580×10^{-8}
Δy	20.39 nm	6.484×10^{-8}	9.812 nm	2.764×10^{-8}	30.2 nm	7.442×10^{-7}
$\Delta\gamma$	2.20 μm	0.305	2.20 μm	0.305	2.20 μm	0.305

used for position control. The control systems and their position control performance are presented in the following section.

6. Position control

A schematic of the controller design is shown in Figure 6. In operation it is desired to control the x, y position of the end-effector in the Cartesian workspace and also to control the orientation, γ, of the end-effector. The reachable workspace of the micromotion stage is ± 14 μm in x-axis, ± 13 μm in y-axis and -765 μrad in z-axis when the input displacement range of PZTs is from 0 to 7 μm. The inverse-Jacobian allows us to calculate the required actuator displacements (Δl_1, Δl_2, Δl_3) to give us a desired (Δx, Δy, $\Delta\gamma$). To achieve the required actuator displacements a closed-loop PI controller is used. This controller uses feedback from strain-gauges mounted to the PZT actuators. The PI controller provides adequate response for point-to-point position control. Given that the PZT actuators can now achieve the desired displacement, the accuracy of the end-effector

Figure 6 Schematic of the control system taken from SIMULINK

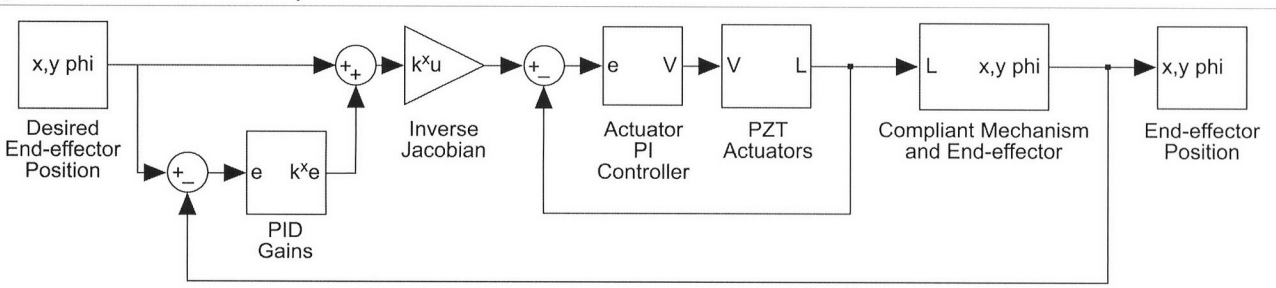

Industrial Robot: An International Journal
Volume 31 · Number 4 · 2004 · 355–361

displacement is dependent on the accuracy of the inverse-Jacobian. The experimentally derived Jacobian is a simple linear constant Jacobian, as given below.

$$\mathcal{J} = \begin{bmatrix} 0.668 & -1.298 & 0.734 \\ -1.183 & -0.0017 & 1.361 \\ -25.433 & -24.975 & -26.073 \end{bmatrix} \quad (5)$$

However, it is possible that there may be some non-linearity in the kinematics, in which case the constant Jacobian may exhibit some inaccuracy. This will result in end-effector positioning errors. To compensate for this error closed-loop end-effector position control was implemented. This uses feedback from the eddy-current sensors and PI gains to compensate for position errors by adjusting the desired input coordinates and orientation of the end-effector.

To demonstrate the performance of the positioning control the end-effector was manoeuvred to 11 random points within the reachable workspace of the micromotion system. The input to the controller was a desired x-y coordinate and an orientation, γ. Two control options were implemented and compared. In the first case actuator feedback only is used. This case has been termed *end-effector open-loop*. In this case the end-effector positioning accuracy is dependent on the accuracy of the Jacobian. In the second case, both actuator and end-effector feedback are used. This case has been termed *end-effector closed-loop*. In this case the position accuracy is limited only by the accuracy of the eddy-current sensors and the performance of the feedback control system. Figure 7 shows the x-y coordinates of the 11 desired points in the workspace and the actual points reached by the end-effector. Table II gives the desired orientations for the end-effector at each of the 11 points and the actual orientation achieved. The absolute orientation errors are also given. Table III gives the average absolute error for x, y and γ for the two controller cases.

7. Conclusions and future work

This paper presents the development of a three-DOF compliant micromotion stage with flexure hinges. This micromotion stage has parallel structure and can be implemented for applications requiring motions in micrometres or even nanometres. Possible applications include microsystem assembly, biological cell manipulation and microsurgery. It is demonstrated in this paper that by using the experimental Jacobian the presented system has achieved good position control. However, the positioning accuracy is significantly improved by incorporating end-effector close-loop control. The authors have observed that the kinematic models that have been derived by various researchers are still inaccurate to predict and analyse the behavior of micromotion systems, even after calibration. Therefore, one direction of future work will be to improve modelling accuracy, while keeping the model as computationally efficient as possible.

Figure 7 Random points showing the desired and actual position of the end-effector for two controller cases

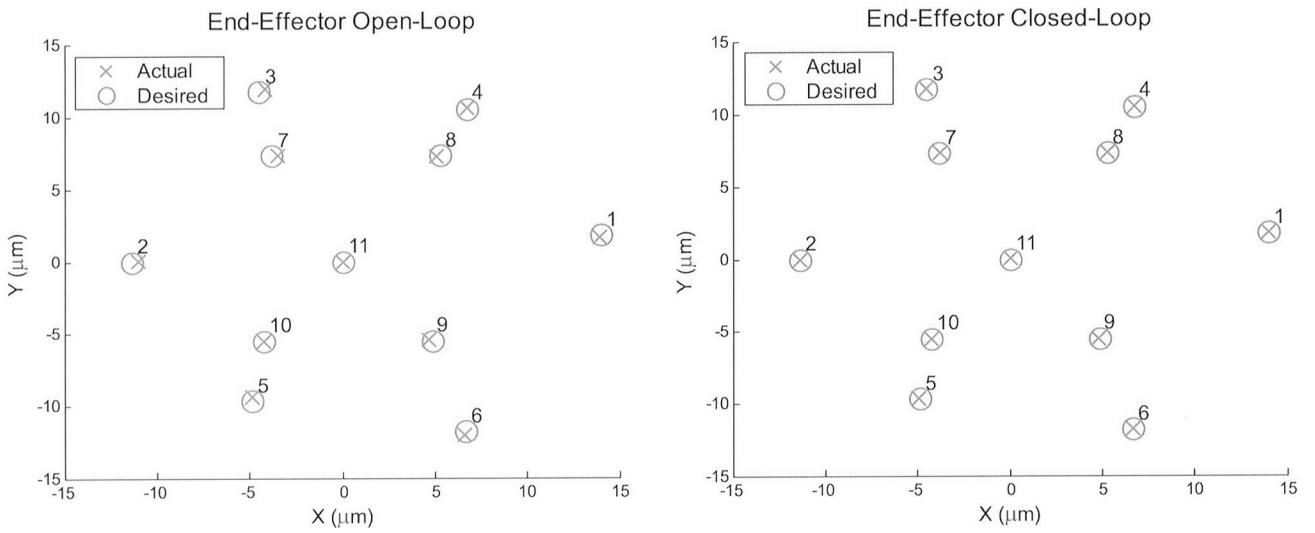

Table II The desired and actual orientation of the end-effector at each of the random points

	End-effector open-loop			End-effector closed-loop		
Points	$\Delta\gamma$ Desired (μrad)	$\Delta\gamma$ Actual (μrad)	Absolute error (μrad)	$\Delta\gamma$ Desired (μrad)	$\Delta\gamma$ Actual (μrad)	Absolute error (μrad)
1	−515.06	−511.14	3.92	−515.06	−515.07	0.01
2	−249.75	−240.98	8.77	−249.75	−249.57	0.18
3	−510.00	−506.47	3.53	−510.00	−510.09	0.09
4	−320.73	−312.09	8.64	−320.73	−320.49	0.24
5	−504.08	−489.95	14.13	−504.08	−503.75	0.33
6	−254.33	−263.43	9.10	−254.33	−254.34	0.01
7	−509.66	−501.88	7.78	−509.66	−509.72	0.06
8	−334.83	−332.14	2.69	−334.83	−334.86	0.03
9	−255.15	−256.64	1.49	−255.15	−255.03	0.12
10	−429.98	−429.92	0.06	−429.98	−429.96	0.02
11	−690.00	−689.88	0.12	−690.00	−690.09	0.09

Table III The average absolute error of x, y and γ for the two controller cases

Average absolute error	End-effector open-loop	End-effector closed-loop
x (μm)	0.15	0.02
y (μm)	0.1	0.01
γ (μrad)	5.48	0.11

Notes

1 R: Revolute
2 Δx and Δy are the translational motions along x- and y-axis, respectively. $\Delta\gamma$ is the rotational motion about the z-axis.

References

Codourey, A. (1998), "Dynamic modeling of parallel robots for computed-torque control implementation", *The International Journal of Robotics Research*, Vol. 17 No. 12, pp. 1325-36.

Gao, P., Swei, S. and Yuan, Z. (1999), "A new piezodriven precision micropositioning stage utilizing flexure hinges", *Nanotechnology*, Vol. 10, pp. 394-8.

Handley, D.C., Lu, T.-F., Yong, Y.K. and Zhang, W.J. (2004), "A simple and efficient dynamic modeling method for compliant micropositioning mechanisms using flexure hinges", *Device and Process Technologies for MEMS, Microelectronics, and Photonics III, Proceedings of SPIE*, Perth, Australia, Vol. 5276, pp. 67-76.

Howell, L. (2001), *Compliant Mechanisms*, Chapter 1, Wiley, New York. NY.

Howell, L.L. and Midha, A. (1996), "A loop-closure theory for the analysis and synthesis of compliant mechanisms", *Journal of Mechanical Design*, Vol. 118, pp. 121-5.

Ma, O. and Angeles, J. (1993), "Direct kinematic and dynamics of a planar three-dof parallel manipulator", *Advances in Design Automation*, Vol. 2, pp. 313-20.

Ryu, J., Gweon, D. and Moon, K. (1997), "Optimal design of a flexure hinge based XYθ wafer stage", *Precision Engineering*, Vol. 21, pp. 18-28.

Scire, F. and Teague, C. (1978), "Piezodriven 50 μm range stage with subnanometer resolution", *Rev. Sci. Instrum*, Vol. 49 No. 12, pp. 1735-41.

Yong, Y.K., Lu, T-F. and Handley, D.C. (2004), "Loop closure theory in deriving a linear and simple kinematic model for a 3 DOF parallel micro-motion system", *Device and Process Technologies for MEMS, Microelectronics, and Photonics III, Proceedings of SPIE*, Perth, Australia, Vol. 5276, pp. 57-66.

Zhang, W.J., Zou, J., Watson, G., Zhao, W., Zong, G. and Bi, S. (2002), "Constant-Jacobian method for kinematics of a 3-DOF planar micro-motion stage", *Journal of Robotic Systems*, Vol. 19 No. 2, pp. 63-79.